

# LEARNING FILL-IN REDUCTION ORDERING VIA GRAPH POLICY OPTIMIZATION FOR SPARSE MATRICES

Ziwei Li<sup>1,2</sup>, Shuzi Niu<sup>1\*</sup>, Huiyuan Li<sup>1\*</sup>, Tao Yuan<sup>1\*</sup>, and Wenjia Wu<sup>1</sup>

<sup>1</sup> Institute of Software, Chinese Academy of Sciences, Beijing, China

<sup>2</sup> University of Chinese Academy of Sciences, Beijing, China

## ABSTRACT

Matrix reordering in large sparse solvers seeks a permutation that minimizes factorization fill-in to reduce memory and computation. Because the minimum fill-in ordering problem is NP-complete and fill-in is implicit in the sparsity pattern, graph-theoretic heuristics are used. Existing reinforcement learning methods either ignore sparsity patterns—missing the global fill-in—or lack local exact fill-in feedback. We propose a graph policy optimization method, modeling fill-ins from global and local views: both the policy and value networks use a multi-hop graph neural backbone to embed global fill-in; the policy further interacts with symbolic factorization over graphs to extract local, step-level fill-ins, and the resulting feedback is aligned with the value network via an adaptive saturation function to improve convergence. On the SuiteSparse Matrix Collection, our method achieves mean reductions of 29.3% in fill-ins and 31.3% in peak memory usage over state-of-the-art baselines.

**Index Terms**— Reinforcement Learning, Graph Neural Network, Matrix Reordering, Fill-in Reduction

## 1. INTRODUCTION

Matrix reordering is a key step that can substantially reduce memory usage when solving sparse linear systems. Many large-scale scientific simulations—such as structural engineering and computational fluid dynamics—lead to large sparse linear systems  $Ax = b$ . A matrix  $A \in \mathbb{R}^{n \times n}$  is sparse when only a small fraction of its entries are nonzero [1], allowing storage and computation to focus on the nonzeros. In practice, one solves these systems by factoring  $A$  as  $A = LU$ , where  $L$  is lower-triangular and  $U$  is upper-triangular. This LU factorization is Gaussian elimination in matrix form, realized via row operations. In sparse settings, the factors  $L$  and  $U$  often contain many more nonzeros than  $A$ ; these new entries are fill-ins, which drive memory and runtime.

The Rose–Tarjan fill path theorem [2] states that fill-ins are generated from the sparsity pattern of the matrix and the elimination ordering. The sparsity pattern of  $A$  is described by its adjacency graph  $G$  with a node for each row/column and an edge for each nonzero (undirected when  $A$  is symmetric). Practically, symbolic factorization is an efficient graphical algorithm that leverages this theorem to predict fill-ins and estimate the memory and computational requirements of the subsequent numerical factorization. An intuitive understanding is illustrated in Fig. 1, showing that eliminating a column in Gaussian elimination corresponds to removing a node and connecting its neighbors into a clique; the new nonzeros correspond to the added edges. Generally, matrix reordering is intrinsically a node reordering problem over the adjacency graph.

However, computing the minimum fill-in ordering problem is NP-complete [2, 3]. Graph-theoretic algorithms rely on heuristics such as node degrees and separators to deduce the node decision per step and finally produce approximate elimination orders. Approximate Minimum Degree (AMD) [4, 5, 6] and Nested Dissection (ND) [7] are representative degree- and separator-based methods, respectively. Such algorithms are usually complex and specially designed for certain kind of matrices.

Deep learning helps obtain a general reordering model. But the learning objective function, the number of fill-ins, is difficult to formalize explicitly and optimize directly. Deep reinforcement learning (DRL) instead minimizes the fill-in number iteratively via environment feedback. One related DRL method DRL-ND [8] uses a graph neural network on the adjacency graph as the node decision agent and learns agent parameters by minimizing node separators. It exploits the sparsity pattern, but was not designed straightly for fill-in minimization. Another related DRL method AlphaElim [9] applies a convolutional neural network over the matrix as the column elimination agent and trains agent parameters by minimizing fill-ins. It takes substantial computation for useless numeric operations and ignores the sparsity pattern. Therefore, we focus on leveraging the sparsity pattern to learn a general reordering agent model by directly optimizing the number of fill-ins.

To solve this problem, we propose Graph Policy Optimization (GPO) for sparse matrix reordering to reduce fill-in. First, we show that fill-ins are generated from the sparsity pattern of the matrix rather than specific numeric values. GPO operates on the adjacency graph of the sparsity pattern to model the entire fill-in generation process. It employs a policy network based on a graph neural network with multi-hop aggregation to choose which node to eliminate next. Crucially, the action is informed by feedback from a theoretically sound symbolic factorization process that calculates the resulting fill-ins. In addition, the value network refines its output via an adaptive saturation function to align with this feedback and stabilize the learning process. We train on sparse matrix benchmarks generated via Delaunay triangulation [10, 8, 9], and evaluate on the SuiteSparse Matrix Collection [11]. Metrics include mean fill-in count and mean peak memory usage during LU factorization, and GPO outperforms graph-theoretic and DRL baselines.

## 2. METHOD

### 2.1. Fill-in Generation

Given a sparse matrix  $A$ , fill-ins arise from matrix factorization, most commonly LU factorization [12, 13, 14]. It is expressed as  $A = LU$  and derived from the Gaussian elimination process.  $L$  and  $U$  are the lower and upper triangular matrices respectively and  $L$  has a unit diagonal  $I$ . For simplicity, we mainly consider the symmetric

\* Corresponding authors: {shuzi, huiyuan, yuantao}@iscas.ac.cn

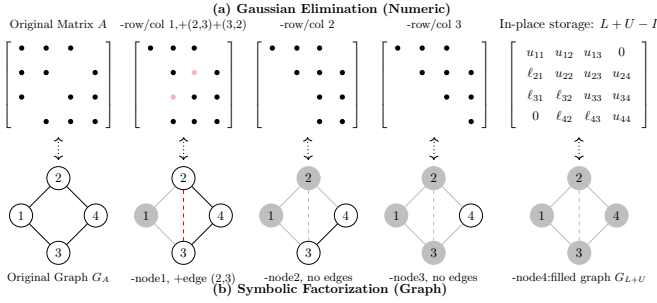


**Fig. 1:** Step-level Fill-ins Generated from Symbolic Factorization

positive definite matrices  $A \in \mathbb{R}^{n \times n}$ . Thus the Cholesky factor  $L$  of matrix  $A$  is a lower triangular matrix satisfying  $A = LL^T$ , where  $L^T$  is the corresponding upper triangular factor  $U$ . The number of nonzero entries in  $A$  is denoted as  $\text{nnz}(A)$ . Fill-ins are defined as new nonzero elements that are in  $L + U - I$  but not in  $A$ .

Fill-ins are completely embedded in sparsity patterns. An  $n \times n$  sparse matrix  $A$  induces an adjacency graph  $G_A = (V_A, E_A)$ : each row/column corresponds to a node  $v \in V_A$ , and each nonzero  $A_{ij} \neq 0$  corresponds to an edge  $e_{ij} \in E_A$ . When  $A$  is symmetric,  $G_A$  is undirected. The Fill-Path Theorem [2] states that an entry  $L_{ij}$  in the factor is nonzero iff there exists a path between  $i$  and  $j$  in  $G_A$  whose internal nodes are eliminated earlier than both  $i$  and  $j$ . Given an elimination order, this theorem allows one to enumerate all potential fill-ins by tracing such connection paths. Symbolic factorization process in Alg.1 is an efficient and precise implementation of this basic idea to predict the fill-in pattern from the adjacency graph.

---

**Algorithm 1** Basic Symbolic Cholesky Factorization Process

---

**Require:** Graph  $G_A$  and Elimination Ordering  $\pi$   
**Ensure:** Fill Patterns  $\mathcal{F}$ ,  
 Filled graph  $G_L$  with the adjacency matrix  $L + L^T$

- 1:  $G_0 \leftarrow G_A$
- 2:  $\mathcal{F} \leftarrow \{\emptyset\}_{k=0}^{n-1}$
- 3: **for**  $k \leftarrow 0$  **to**  $n - 1$  **do**
- 4:    $v \leftarrow \pi(k)$
- 5:    $N_v^{(k)} \leftarrow \{u \mid (u, v) \in E_k\}$
- 6:   **for**  $u \in N_v^{(k)}$  **do**
- 7:     **for**  $w \in N_v^{(k)} - \{u\}$  **do**
- 8:      **if**  $(u, w) \notin E_k$  **then**
- 9:        $\mathcal{F}_k \leftarrow \mathcal{F}_k \cup \{(u, w)\}$
- 10:      **end if**
- 11:    **end for**
- 12:   **end for**
- 13:    $G_{k+1} \leftarrow (V_k - \{v\}, (E_k - N_v^{(k)} \times \{v\}) \cup \mathcal{F}_k)$
- 14: **end for**
- 15:  $\mathcal{F} \leftarrow \cup_{k=1}^n \mathcal{F}_k$
- 16:  $G_L \leftarrow (V_0, E_0 \cup \mathcal{F})$

---

Given an elimination ordering  $\pi$  and the adjacency graph  $G_A$ , fill-ins are predicted by sequentially eliminating nodes as Alg.1. When the  $k$ -th node in the ordering,  $v = \pi(k)$ ,  $0 \leq k \leq n - 1$ , is eliminated from the current graph  $G_k = (V_k, E_k)$ , namely elimination graph, edges connected to  $v$  will be removed, denoted by  $N_v^{(k)} \times \{v\}$ , where  $N_v^{(k)}$  is  $v$ 's neighbor set [15]. At the same time, additional edges  $\mathcal{F}_k$  will be added among node pairs in  $N_v^{(k)}$ , where there are no edges in the current graph  $G_k$ . Each fill edge  $(u, w)$ ,  $u, w \in N_v^{(k)}$  naturally satisfies the condition that the elimi-

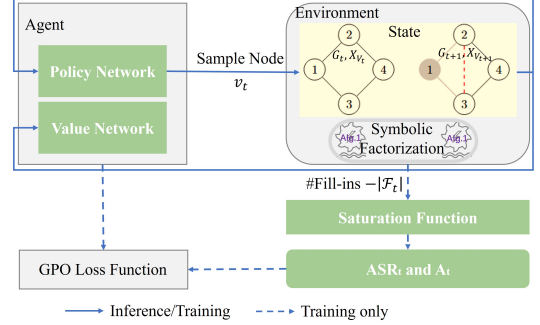


**Fig. 2:** Architecture of the Graph Policy Optimization Framework

nation orders of  $u$  and  $w$  are greater than  $k$ . In addition to  $\mathcal{F}_k$ , the elimination graph will be updated as  $G_{k+1}$  according to Line 13 of Alg.1 and the subgraph of  $N_v^{(k)}$  will become a clique. We repeat this elimination process  $n$  times until all nodes have been removed. Ultimately, the fill-ins generated throughout the entire elimination process can be expressed as  $\cup_{k=0}^{n-1} \mathcal{F}_k$ . For a specific graph, different orderings lead to different fill-ins. In this sense, matrix reordering is to find an elimination ordering  $\pi$  over the adjacency graph  $G_A$  to minimize the number of generated fill-ins  $|\cup_{k=0}^{n-1} \mathcal{F}_k|$ .

## 2.2. Graph Policy Optimization Framework

We propose a Graph Policy Optimization (GPO) framework to learn effective node elimination policies that minimize fill-ins in Fig. 2. With reinforcement learning, GPO addresses the non-differentiability of the fill-in objective. Fill-ins are exactly collected from the interaction between GNN agent and the symbolic factorization process on the adjacency graph per node elimination step. The policy and value network parameters with MixHopConv backbones are learned by minimizing the adaptive saturation version of fill-ins.

We adopt a reinforcement learning formulation with the following components. **The environment** is the symbolic factorization process illustrated in Alg. 1. **The state** at time step  $t$  is the elimination graph  $G_t = (V_t, E_t)$  together with its node features  $X_{V_t}$ . The node features are the node degree in  $G_t$ ,  $\text{deg}(v)$ , and collective influence [16] in Eq.(1).  $\text{CI}(v) = (\text{deg}(v) - 1) \sum_{u \in N(v)} (\text{deg}(u) - 1)$ . **The state space** comprises all elimination graphs and their associated node features that can be generated under different node-elimination orders. **The action space** consists of all nodes  $V_A$  in the original graph  $G_A$ ; at time step  $t$ , the action is chosen from the nodes  $V_t$  in the current elimination graph  $G_t$ .

$$\text{CI}(v) = (\text{deg}(v) - 1) \sum_{u \in N(v)} (\text{deg}(u) - 1) \quad (1)$$

**The agent** consists of a policy and value network illustrated in Fig. 3. The policy network takes the elimination graph  $G_t$  and the node-feature matrix  $X_{V_t}$ , and outputs a log-probabilities  $\pi(V_t | G_t)$  over candidate nodes for elimination. The value network computing a scalar  $\text{Value}(G_t)$  as the expected average adaptive saturation return achievable from  $G_t$ . Both networks are composed of several MixHopConv layers [17] with tanh activation functions to extract meaningful node embeddings. The key difference lies in the final transformation layer. For the actor network, the output from the last tanh activation is passed through a linear transformation followed by a log\_softmax layer, producing the probability distribution for node selection. In contrast, for the critic network, a linear transformation is applied before the final tanh activation to generate a representation of the graph, which is used to evaluate the current state. At each time step, the agent selects a node to eliminate according to  $\pi(V_t | G_t)$

and performs the elimination as in Alg. 1, which yields a **state transition**  $G_t \rightarrow G_{t+1}$ .

$$\text{ASR}_t(|E_t|, R_t) = \frac{|E_t| + R_t}{|E_t| - R_t} \quad (2)$$

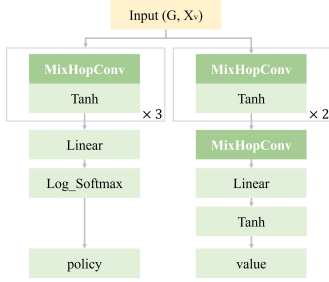


Fig. 3: Network Architecture of GNN-Agent

The reward  $r_t$  is defined as the negative count of added edges,  $r_t = -|\mathcal{F}_t|$ . To reduce variance and make training more stable, the **Adaptive Saturation Return** normalizes the number of fill-ins as Eq.(2). where  $|E_t|$  is the number of edges in  $G_t$ , and  $-R_t$  is the number of newly added edges from time  $t$  to termination, i.e.,  $R_t = \sum_{k=t}^{n-1} r_k$ . The **advantage function** is defined as the difference between the adaptive saturation return and the value function,  $A_t = \text{ASR}_t - \text{Value}(G_t)$ ; it measures how much better the selected action is relative to the expected return. The actor loss  $L_a$  is defined as the negative sum of log probabilities multiplied by their respective advantages in Eq.(3). The critic loss  $L_c$  is designed as the mean squared error between the adaptive saturation returns and the state value estimates in Eq.(3). GPO training process is in Alg. 2.

$$L_a = -\frac{1}{n} \sum_{t=0}^{n-1} \pi(v_t|G_t) \cdot A_t, L_c = \frac{1}{n} \sum_{t=0}^{n-1} A_t^2 \quad (3)$$

---

#### Algorithm 2 Graph Policy Optimization Training Process

---

**Require:** Training Graph Set  $\{G\}$

- 1: **for** each graph  $G$  in  $\{G\}$  **do**
  - 2:   Initialize  $G_0 = G, X_V$
  - 3:   Initialize policies  $\mathcal{P} = \square$ , values  $\mathcal{V} = \square$
  - 4:   Initialize rewards  $\mathcal{R} = \square$ , the number of edges  $\mathcal{E} = \square$
  - 5:   **for**  $t$  from 0 to  $n - 1$  **do**
  - 6:      $\pi(V_t|G_t), \text{Value}(G_t) \leftarrow \text{GNN}(G_t, X_{V_t})$
  - 7:     Sample node  $v_t$  from policy distribution  $\pi(V_t|G_t)$
  - 8:      $\mathcal{P}.\text{append}(\pi(v_t|G_t)), \mathcal{V}.\text{append}(\text{Value}(G_t))$
  - 9:     // eliminate the node, calculate fill-ins and  $X_{V_t}$
  - 10:     $G_{t+1}, \mathcal{F}_t, X_{V_{t+1}} \leftarrow \text{NodeElimination}(G_t, v_t)$
  - 11:     $\mathcal{R}.\text{append}(-|\mathcal{F}_t|), \mathcal{E}.\text{append}(|E_t|)$
  - 12:   **end for**
  - 13:   Compute the Adaptive Saturation Return  $\text{ASR}(\mathcal{E}, \mathcal{R})$
  - 14:   Compute the advantages  $\mathcal{A} = \text{ASR} - \mathcal{V}$
  - 15:   Compute the loss per episode  $L_{actor}$  and  $L_{critic}$
  - 16:   UpdateGNNParameters( $L_{actor}, L_{critic}$ )
  - 17: **end for**
- 

The whole updating step for each training graph  $G$  is from Line 2 to 16 of Alg. 2. It includes initialization from Line 2 to 4, inference process along with fill-in collection from Line 5 to 12, and gradient backpropagation from Line 13 to 16. The initial state of the environment is represented as  $G_0 = G$  together with its node features

Table 1: Test Matrix Count Distribution by Matrix Type and Size

Data set	S(10-500)	M(500-1k)	L(1k-10k)	XL(10k-100k)	Total
SP	24	20	30	10	84
2D/3D	14	14	10	10	48
CSP	6	—	19	9	34
EP	8	7	14	6	35
CFDP	22	23	70	16	131

$X_V$ . Both the agent inference process and fill-in collection process are interleaved within Line 5~12. For a new test graph, its complete elimination ordering is derived from  $\mathcal{P}$  after running Line 5~12.

## 3. EXPERIMENTS

### 3.1. Experimental Settings

As training data, we generate 10,000 symmetric matrices via Delaunay triangulation [10, 9, 8] with sizes  $n \in [60, 200]$ . For evaluation, we randomly sample from each category of the SuiteSparse Matrix Collection to form a 332-matrix test set spanning five domains: Structural Problem (SP), 2D/3D Problem (2D/3D), Circuit Simulation Problem (CSP), Electromagnetics Problem (EP), and Computational Fluid Dynamics Problem (CFDP). Sizes are grouped as S (10–500), M (500–1k), L (1k–10k), and XL (10k–100k), where “size” denotes the number of rows/columns; unsymmetric matrices are evaluated on the symmetrized form  $A + A^T$ . The test matrix distribution is in Table 1. Each MixHopConv layer is of 16 hidden units. We implement GPO with PyTorch and Adam optimizer with learning rate 0.01 for epoch 1 and 0.001 thereafter. Training phase is completed in 50 hours on an NVIDIA A100.

### 3.2. Evaluation Protocols

We compare GPO with Natural Ordering and two representative classical graph-theoretic baselines—COLAMD [6] and ND (implemented via METIS [18] and referred to as METIS)—plus three RL baselines: (i) *PPO*, obtained by replacing GPO’s A2C-like loss with a PPO-style loss under identical training data and hyperparameters; (ii) *DRL-ND* [8], which learns graph partitions to minimize normalized node separators and then applies graph-theoretic reorderings within each subgraph (trained exactly as in [8]); and (iii) *AlphaElim* [9], which treats the matrix as an image and combines CNNs with MCTS to align the reordering process with the numerical factorization steps of Gaussian elimination. To improve parallelism on large problems, we partition  $G_A$  using Nested Dissection and run GPO on each subgraph when the matrix size exceeds  $10^3$ .

For each test matrix  $A$ , we compute an ordering with each method, apply it to obtain  $A'$ , and factorize  $A'$  using `splu`, a Python interface for SuperLU [19], to produce  $L$  and  $U$ . We report the fill-in ratio  $\text{FIR} = \frac{\text{nnz}(L+U-I) - \text{nnz}(A)}{\text{nnz}(A)}$ , which normalizes the extra nonzeros by the original sparsity so matrices of different sizes and densities are comparable. We also report the peak memory during factorization—the maximum resident set size in kilobytes (PM\_KB)—capturing the footprint of the factors and all work arrays.

### 3.3. Memory Usage Analysis of LU Factorization

For each of the 19 matrix groups in Table 1, Table 2 shows the average fill-in ratio for each reordering method, excluding AlphaElim. Since the source code of AlphaElim [9] is unavailable, it is evaluated separately at the end of this subsection. To better illustrate the impact of reordering on memory usage during LU factorization, we

**Table 2:** Fill-in Ratio of Sparse Matrix Reordering Algorithms on SuiteSparse Test Set

Algorithm	2D/3D Problem				Structural Problem				Circuit Simulation Problem				Computational Fluid Dynamics				Electromagnetics Problem			
	S	M	L	XL	S	M	L	XL	S	M	L	XL	S	M	L	XL	S	M	L	XL
NATURAL	5.5391	21.4712	37.6738	131.201	5.3414	11.0633	26.6641	53.151	10.5513	-	200.05	723.78	3.7866	9.1709	15.3802	166.45	8.1252	23.4617	26.3767	369.265
COLAMD	1.8089	4.0584	5.3278	29.6666	2.0060	2.9777	5.0403	20.761	1.0625	-	30.995	44.387	1.7982	4.1578	5.6925	16.243	0.8596	3.3734	4.8695	60.6559
METIS	1.3055	3.0115	<b>3.2885</b>	<b>11.6896</b>	1.3021	2.3826	3.1239	9.6555	0.5628	-	6.4704	3.3489	1.2606	2.7999	3.2052	10.011	0.9679	3.0492	3.4340	21.3862
DRL_ND	1.8362	5.1762	4.0304	14.6448	1.3647	2.6048	5.7978	13.237	0.7011	-	6.9841	4.7575	1.5166	3.5259	4.7636	25.670	1.1079	4.2830	7.4880	27.7424
PPO	1.6532	4.6778	3.4141	12.0328	2.3061	5.1168	3.3386	10.052	0.5438	-	6.3444	3.7386	2.0351	4.7473	3.4806	10.445	1.2033	3.6963	3.6507	21.6282
GPO	<b>1.1063</b>	<b>2.6354</b>	3.3353	11.9360	<b>1.2269</b>	<b>2.3053</b>	<b>3.0499</b>	<b>9.4997</b>	<b>0.4866</b>	-	<b>6.2848</b>	<b>3.0067</b>	<b>0.9872</b>	<b>2.3636</b>	<b>3.1227</b>	<b>9.9480</b>	<b>0.7630</b>	<b>2.6253</b>	<b>3.4176</b>	<b>20.9969</b>

**Table 3:** Nonzero Number nnz(L+U) and Peak Memory Usage in Kilobytes (PM\_KB) of LU Factorization with Different Reordering Methods

Matrix	Size(n)	NATURAL		COLAMD		METIS		DRL_ND		PPO		GPO	
		nnz(L+U)	PM_KB	nnz(L+U)	PM_KB	nnz(L+U)	PM_KB	nnz(L+U)	PM_KB	nnz(L+U)	PM_KB	nnz(L+U)	PM_KB
Pres_Poisson	14,822	10,229,633	273,888	5,504,778	183,176	4,996,318	158,736	5,896,452	186,148	5,259,803	165,832	<b>4,735,200</b>	<b>154,176</b>
besstk31	35,588	46,538,357	1,102,056	23,055,939	577,872	10,506,668	291,004	13,527,311	360,360	10,046,738	279,132	<b>9,777,728</b>	<b>273,484</b>
besstk36	23,052	20,624,794	528,192	14,112,629	383,308	10,933,097	306,324	10,536,260	296,024	8,796,149	256,880	<b>7,674,468</b>	<b>235,144</b>
coupled	11,341	40,547,108	1,008,928	1,067,616	65,824	1,066,795	63,684	59,412	479,395	1,019,026	62,548	<b>426,787</b>	<b>48,672</b>
pli	22,695	40,322,762	977,908	57,276,921	1,313,628	38,350,240	895,148	54,505,246	1,245,588	38,599,143	901,276	<b>35,082,796</b>	<b>819,808</b>
poisson3Da	13,514	166,114,198	3,653,376	15,177,132	378,388	5,617,200	167,004	6,161,232	187,800	5,643,660	167,184	<b>5,374,060</b>	<b>161,768</b>

**Table 4:** Fill-in Ratio Comparison between AlphaElim and GPO

Matrix	Size (n)	FIR(AlphaElim)	FIR(GPO)
mbeause	496	<b>1.3101</b>	1.3123
olm500	500	0.5381	<b>0.0000</b>
ex27	974	<b>0.6984</b>	0.7165
m.tl	97578	-0.2415	5.4822
tx2010	914231	290.7237	<b>3.4145</b>
Hardesty1	938905	39.3514	<b>16.7099</b>

also report peak memory usage (PM\_KB) for a subset of matrices with  $n > 10,000$ , randomly sampled from the matrices listed in Table 1. Results are shown in Table 3.

As shown in Table 3, PM\_KB decreases as the fill-in drops, indicating lower peak working set during factorization. In Tables 2 and 3, all reordering methods outperform Natural Ordering in both FIR and PM\_KB, underscoring the value of reordering. GPO consistently achieves the lowest FIR and the lowest PM\_KB across problem domains, attributable to alignment with symbolic factorization, MixHopConv GNN as backbone and proposed adaptive saturation return. One exception is that GPO exhibits a slightly higher fill-in ratio than METIS on the large and extra-large 2D/3D matrices. The reason lies in that the graph partitioning method has more effect on the fill-in ratio for large 2D/3D matrices.

Reinforcement-learning methods achieve state-of-the-art results versus graph-theoretic baselines on most matrices in both metrics, highlighting the suitability of RL-based reorderings. Although training uses only Delaunay-triangulation matrices while testing uses real SuiteSparse matrices with markedly different sizes and sparsity patterns, the lower FIR and PM\_KB on the test set indicate strong generalization, especially for GPO. Moreover, despite being trained on small matrices ( $n \in [60, 200]$ ), we do not partition test matrices with  $n \leq 1,000$  (S/M categories) and reorder them directly; even so, GPO attains the lowest FIR, demonstrating scalability.

We restrict the comparison to matrices evaluated by AlphaElim (Table 4). FIR(AlphaElim) is computed from its reported nonzero counts. From table, GPO performs comparably to AlphaElim on small matrices with  $n < 1,000$ , and even outperforms it on olm500. For large-scale matrices with sizes approaching one million, GPO demonstrates significantly better fill-in reduction. However, the result on matrix m.tl appears unusual: AlphaElim yields a negative fill-in ratio, which is counterintuitive considering the unstructured numerical values of the matrix. In all, results indicate that GPO achieves superior performance compared to AlphaElim, particularly on large-scale sparse matrices.

Overall, compared with state-of-the-art baselines (excluding Natural Ordering and AlphaElim), GPO achieves a **29.3%** mean reduction in fill-in ratio. For matrices with  $n > 10,000$ , it further re-

**Table 5:** Ablation Study in Terms of Fill-in Ratio on 2D3D Problem

	DRL_SF	DRL_ND	↑	GPO	GPO_SAGE	↑
2D3D-S	<b>1.2306</b>	1.8362	-0.6056	<b>1.1063</b>	1.1147	-0.0084
2D3D-M	6.2428	<b>5.1762</b>	1.0666	<b>2.6354</b>	5.5880	-2.9526
2D3D-L	<b>3.3438</b>	4.0304	-0.6866	<b>3.3353</b>	3.3370	-0.0017
2D3D-XL	<b>11.9553</b>	14.6448	-2.6895	<b>11.9360</b>	11.9370	-0.0010

duces PM\_KB by an average of **31.13%**. These reductions translate into a smaller working set during LU factorization, which is critical for large-scale sparse computations.

### 3.4. Ablation Study

Here we study the roles of two key components in GPO including MixHopConv backbone and the symbolic factorization process. To explore the role of agent backbone, we replace MixHopConv with the SAGEConv [20] in GPO denoted as GPO.SAGE. To probe into the reinforcement learning process, we keep the agent backbone in DRL\_ND, change its alignment with nested dissection into alignment with Symbolic Factorization, which we refer to as DRL\_SF.

Comparing GPO and GPO.SAGE in Table 5, results indicate that the MixHopConv backbone has a positive effect on the reordering method. Global context modeling in MixHopConv is helpful especially for large sparse matrices. DRL\_SF consistently achieves a lower fill-in ratio than DRL\_ND, except for medium-sized sparse matrices. As the matrix size increases, the fill-in ratio discrepancy increases. It suggests the excellent effect of alignment with symbolic factorization on larger sparse matrices. Both components are essential for fill-in reduction of GPO.

## 4. CONCLUSION

Sparse matrix reordering seeks an elimination ordering that minimizes fill-ins during matrix factorization. To avoid costly numerical factorization and leverage graph structures, we analyze the correspondence between symbolic and numerical factorization and establish that fill-in depends on the original graph and the elimination order. To address the lack of an explicit fill-in formulation while capturing both global graph context and local fill-in pattern, we propose a reinforcement learning-based Graph Policy Optimization framework. It models symbolic factorization as environment dynamics, using the negative number of fill-ins as the reward. MixHopConv GNNs serve as actor-critic backbones to alleviate locality limitations. Experiments on real-world sparse matrices show that our method outperforms graph-theoretic and reinforcement learning baselines in both fill-in ratio and peak memory usage.

## 5. ACKNOWLEDGMENTS

This research was supported by the National Key R&D Program of China under Grant No. 2021YFB0300203.

## 6. REFERENCES

- [1] J.H. Wilkinson and C. Reinsch, *Handbook for Automatic Computation: Volume II: Linear Algebra*, vol. 186 of *Die Grundlehren der mathematischen Wissenschaften, in Einzeldarstellungen mit besonderer Berücksichtigung der Anwendungsgebiete*, Springer Berlin Heidelberg, Berlin, Heidelberg, 1971.
- [2] Donald J. Rose, Robert E. Tarjan, and George S. Lueker, “Algorithmic aspects of vertex elimination,” *SIAM Journal on Computing*, vol. 5, no. 2, pp. 266–283, 1976.
- [3] M. Yannakakis, “Computing the minimum fill-in is np-complete,” *SIAM Journal on Algebraic Discrete Methods*, vol. 2, no. 1, pp. 77–79, 1981.
- [4] D.J. Rose, “A graph-theoretic study of the numerical solution of sparse positive definite systems of linear equations,” *Graph theory and computing*, pp. 183–217, 1972.
- [5] Patrick R. Amestoy, Timothy A. Davis, and Iain S. Duff, “An approximate minimum degree ordering algorithm,” *SIAM Journal on Matrix Analysis and Applications*, vol. 17, no. 4, pp. 886–905, 1996.
- [6] Timothy A. Davis, John R. Gilbert, Stefan I. Larimore, and Esmond G. Ng, “A column approximate minimum degree ordering algorithm,” *ACM Transactions on Mathematical Software*, vol. 30, no. 3, pp. 377–380, 2004.
- [7] J. Alan George, “Nested dissection of a regular finite element mesh,” *SIAM Journal on Numerical Analysis*, vol. 10, no. 2, pp. 345–363, 1973.
- [8] Alice Gatti, Zhihui Hu, Tess Smidt, and Pieter Ghysels, “Graph partitioning and sparse matrix ordering using reinforcement learning and graph neural networks,” in *Journal of Machine Learning Research*. 2022, JMLR.org.
- [9] Arpan Dasgupta and Pawan Kumar, “Alpha elimination: Using deep reinforcement learning to reduce fill-in during sparse matrix decomposition,” in *Joint European Conference on Machine Learning and Knowledge Discovery in Databases*. 2023, Springer.
- [10] Ilay Luz, Meirav Galun, Haggai Maron, Ronen Basri, and Irad Yavneh, “Learning algebraic multigrid using graph neural networks,” in *Proceedings of the 37th International Conference on Machine Learning*. 2020, vol. 119, pp. 6489–6499, PMLR.
- [11] Timothy A. Davis and Yifan Hu, “The university of florida sparse matrix collection,” *ACM Transactions on Mathematical Software (TOMS)*, vol. 38, no. 1, pp. 1–25, 2011.
- [12] Alan George and Joseph W.H. Liu, *Computer Solution of Large Sparse Positive Definite*, Prentice-Hall, 1981.
- [13] Iain S. Duff, Albert M. Erisman, and John K. Reid, *Direct Methods for Sparse Matrices*, Clarendon Press, Oxford, 1986.
- [14] Timothy A. Davis, Sivasankaran Rajamanickam, and Wisam M. Sid-Lakhdar, *A Survey of Direct Methods for Sparse Linear Systems*, vol. 25 of *Acta Numerica*, Cambridge University Press, 2016.
- [15] J.W.H. Liu, “The role of elimination trees in sparse factorization,” *SIAM Journal on Matrix Analysis and Applications*, vol. 11, no. 1, pp. 134–172, 1990.
- [16] F. Morone, B. Min, L. Bo, R. Mari, and H. A. Makse, “Collective influence algorithm to find influencers via optimal percolation in massively large social media,” *Scientific Reports*, vol. 6, 2016.
- [17] Sami Abu-El-Haija, Bryan Perozzi, Amol Kapoor, Nazanin Alipourfard, Kristina Lerman, Hrayr Harutyunyan, Greg Ver Steeg, and Aram Galstyan, “Mixhop: Higher-order graph convolutional architectures via sparsified neighborhood mixing,” in *Proceedings of the 36th International Conference on Machine Learning*, Kamalika Chaudhuri and Ruslan Salakhutdinov, Eds. 09–15 Jun 2019, vol. 97 of *Proceedings of Machine Learning Research*, pp. 21–29, PMLR.
- [18] George Karypis and Vipin Kumar, “Metis, a software package for partitioning unstructured graphs, partitioning meshes, and computing fill-reduced orderings of sparse matrices,” Tech. Rep., University of Minnesota, Minneapolis, MN, USA, 1998.
- [19] X. S. Li, “An overview of superlu: Algorithms, implementation, and user interface,” *ACM Transactions on Mathematical Software*, vol. 31, no. 3, pp. 302–325, 2005.
- [20] W. Hamilton, Z. Ying, and J. Leskovec, “Inductive representation learning on large graphs,” in *Advances in Neural Information Processing Systems*, 2017, pp. 1024–1034.